JSTR
ASEAN Journal of Scientific and Technological Reports

Research article

The Differences of Precipitation Characteristics among GCMs over Southeast Asia under AR6 Climate Change Scenarios

Ketvara Sittichok[1*] and Chaiyapong Theppprasit[1]

[1] Department of Irrigation Engineering, Faculty of Engineering at Kampahengsaen Campus, Kasetsart University, Bangkok, 10900, Thailand; fengkrs@ku.ac.th
[1] Department of Irrigation Engineering, Faculty of Engineering at Kampahengsaen Campus, Kasetsart University, Bangkok, 10900, Thailand; fengcpth@ku.ac.th
* Correspondence: E-mail: fengkrs@ku.ac.th

Abstract: Southeast Asia is known globally as a highly vulnerable climate change region. Precipitation is the primary factor that impacts livelihood in this region due to recurring flood and drought incidents. Variables projections under climate change can be made using General Circulation Models (GCMs). An investigation of projected precipitation with the new phase of the model experiment, the Sixth Assessment Report (AR6), is worth to be considered. This study investigates the spatial distributions of variability, trend and conditions (wet/dry) of precipitations generated using 10 GCMs over the SEA under AR6 with four scenarios (SSP1-2.6, SSP2-4.5, SSP3-7.0, and SSP5-8). Three statistical methods, coefficient of variation (CV), Mann-Kendall test (MK) and standardized anomaly index (SAI), were calculated by grid cells. Significant differences among GCMs could be seen in the results. High precipitation variation with CV was indicated around the southern part of Indonesia and the Philippines oceans for six models, whereas only one model (MRI-ESM2) returned strong variation for mainland countries. A decreasing precipitation trend during the historical period could be observed in mainland countries with four GCMs. However, the SSP3-7.0 and SSP5-8.5 of most models presented precipitation increment. The extremely wet and dry ratio to all other years was calculated. Highly wet years higher than 10% were indicated in SSP5-8.5 with MPI-ESM1 occurring in most areas of the region, whereas other models gave 6-10% of highly wet occurrence. Drought situation occurred higher than 10% and could be seen with only three models with small areas under all scenarios.

Keywords; Climate Change; Coefficient of Variation; Mann-Kendall; Standardized Anomaly Index; Southeast Asia; Sixth Assessment Report

Citation:
Sittichok, K.; Theppprasit, S. The Differences of Precipitation Characteristics among GCMs over Southeast Asia under AR6 Climate Change Scenarios . *ASEAN J. Sci. Tech. Report.* **2022**, *25(1)*, 11-23. https://doi.org/10.55164/ajstr.v25i1.244632.

Received: July 12, 2021
Revised: December 20, 2021
Accepted: December 20, 2021
Available online: March 3, 2022

1. Introduction

Southeast Asia (SEA) comprises eleven countries, which are: Indonesia, Myanmar, Thailand, Vietnam, Malaysia, Philippines, Laos, Cambodia, East Timor, Brunei and Singapore. This region is indicated as highly vulnerable to climate change [1,2]. SEA's livelihood mainly relies on agriculture. Therefore, meteorological changes, especially precipitation and temperatures, are

conducive to the growth of agricultural products that factor into the gross domestic product of various countries. These countries are indicated as vulnerable regions to climate change due to most people depending on natural resources [3]. A higher frequency of extreme events resulting in severe droughts and floods, including tropical cyclones, occur in this region, creating high-risk conditions. In addition, 563 million people of this region are located along coastlines around 173,251 kilometres that are at risk of rising sea levels and the impact of tropical storms. Further, this region is likely to face a more significant impact from climate change than the rest of the world [1].

The Intergovernmental Panel on Climate Change (IPCC) launched a new phase of the model experiment, the Sixth Assessment Report (AR6). Nine Shared Socioeconomic Pathways (SSPs) are indicated in the report with five high priority scenarios in Tier 1, comprising four groups (SSP1, SSP2, SSP3 and SSP5). SSP1 is a low challenges group presenting in Tier 1 with two scenarios; SSP1-1.9 and SSP1-2.6. These two scenarios reflect a 1.5 ^{0}C that is an ultimate goal under the Paris Agreement and a 2.0 ^{0}C presenting a sustainability corresponding to the previous scenario RCP 2.6. The middle of the road can be found in SSP2-4.5, presenting closely to the RCP4.5 of the AR5 scenario. SSP3-7.0 and SSP5-8.5 scenarios reflect a medium-high range, up to the highest level of AR6. SSP3-7.0 is in the regional rivalry of the socio-economic family, whereas SSP5-8.5 indicates a high emission scenario relating to the large use of fossil fuels of the 21st century [4].

To gain knowledge about climate change responses to climate systems. General Circulation Models (GCMs) that are the main tools for climate change works were employed. These models can develop climate projections related to future greenhouse gas emissions and socio-economic scenarios. The 50 GCMs and more than 20 institutions collaborate on the Coupled Model Intercomparison Project (CMIP6). For the 6th phase, the climate models, the atmosphere-ocean general circulation models (AOGCMs) and the Earth system models (ESM) calculate the future scenario projections using the concentration of greenhouse gases from all non-CO_2 [4]. Although the projection outputs generated from all GCMs mostly agree in the overview, the regional details among those GCMs should be considered. The differences between models result from various factors such as the model calculations, variability of climate systems and the implication of socio-economic relevance applied in the model. For these reasons, model variations can be noticeably observed; for example, some GCMs may result in dry conditions in a specific region while others may present wet incidents [5].

Precipitation fluctuation in both amount and trend on different temporal and spatial scales has been of great concern for policymakers given its impact on people's livelihood [6], especially in the SEA mentioned above. Drought and flood events are also strongly related to the magnitude of precipitation. An overview investigation of precipitation characteristics over this region should be worthy of notice for the new launch AR6 scenarios before the following model selection and downscaling process. Therefore, this study aims to investigate the differences of original GCM outputs to understand their precipitation characteristics: variations, trends and conditions under AR6 climate change scenarios. Ten available GCMs with only resolution around 100 km for all four scenarios in Tier 1 during 2015-2100 and historical simulations between 1850 and 2014 in the spatial scale of each grid cell were analyzed. Three statistical methods were employed in this study: coefficient of variation (CV), Mann-Kendall method (MK) and standardized anomaly Index (SAI). This research clearly defined the spatial differences of precipitation characteristics of all models and across the entire SEA.

2. Materials and Methods

2.1 Study area

Of the 11 countries in the SEA, 5 (Thailand, Burma, Laos, Cambodia, and Vietnam) are located on the mainland, an extension of the Asian continent. At the same time, the other 6 are island formations (Figure 1). The region is in a tropical zone, and similarities in climate can be found for all countries throughout the region. The agricultural sector is the main source of livelihood in most countries of this area, especially given that there has been a significant increase of land conversion from non-agricultural areas such as grasslands, forest areas and wetlands to cropland for higher yield productivities. Thus, these countries' GDPs have become even more vulnerable to climate change [1].

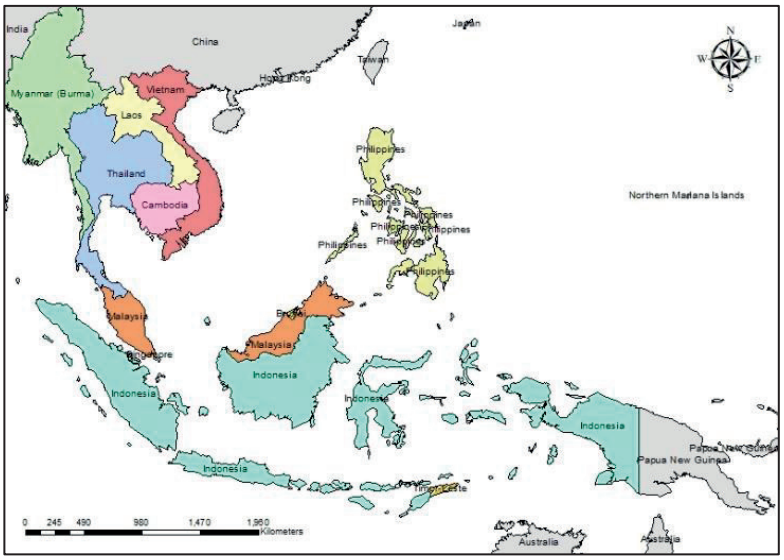

Figure 1. Countries in South East Asia

2.2 Data collection

Projected daily precipitation of four scenarios in Tier 1 (SSP1-2.6 SSP2-4.5 SSP3-7.0 and SSP5-8.5) during 2015-2100, including precipitation in the historical period (1850-2014) in CMIP6 generated from 10 GCMs were modelled. All selected GCMs are the Atmospheric-Ocean General Circulation Models (AOGCMs), which comprises biogeochemical function, for example, vegetation and some atmospheric chemistry in the model [4]. The differences among these 10 GCMs are the main components: land-ocean interactive dynamics, marine biological chemistry, and surface wave functions used to simulate atmospheric and hydrologic variables. The name of the models and their institutions are presented in Table 1. Only GCMs available for all four scenarios, including historical data, are considered in this study. These selected models have resolutions around 100 km. Only variant label of r1i1p1f1 where r, i, p and f refer to realization index, initialization index, physics index and forcing index respectively was selected.

Table 1 Selected GCMs used in this study

GCM	Institution	Abbreviation
CESM2-WACCM	National Center for Atmospheric Research, USA	CESM2
CMCC-CM2-SR5	Euro-Mediterranean Centre on Climate Change coupled climate model	CMCC-CM2
CMCC-ESM2	Euro-Mediterranean Centre on Climate Change coupled climate model	CMCC-ESM2
NorESM2-MM	Norwegian Earth System Model	NorESM2
TaiESM1	Taiwan Earth System Model	TaiESM1
MRI-ESM2-0	The Meteorological Research Institute, Japan	MRI-ESM2
GFDL-ESM4	Geophysical Fluid Dynamics Laboratory, USA	GFDL
INM-CM4-8	The Institute for Numerical Mathematics, Russia	INM-CM4
INM-CM5-0	The Institute for Numerical Mathematics, Russia	INM-CM5
MPI-ESM1-2-HR	The Max Planck Institute for Meteorology, Germany	MPI-ESM1

2.3 Statistical tests

This study employed three statistical methods widely used to estimate precipitation characteristics that were the coefficient of variation (CV), the Mann-Kendall test (MK) and the standardized anomaly index (SAI). The first and second methods were normally used to calculate variations and trends of precipitation based on the specific period. The last one can specify wet/dry years occurrences under the period of interest. Details of each method are presented below.

2.3.1 Coefficient of variation

The coefficient of variation (CV) is a statistic measure index used in this study to estimate rainfall variability. This index benefits to indicate which regions are facing the fluctuation of rainfall, leading to potentially high vulnerability for drought and water scarcity [7]. This method calculates the standard deviation of the rain averaged in a specific period. The CV range is between 0-100% and is classified into three groups. A region presents a CV value less than 20%, indicating low rainfall variability; 20-30% of CV and higher than 30% present medium and high rainfalls variability, respectively [8]. CV was widely used to investigate rainfall variability in various regions [9-11]. This indicator is computed as Equation 1, where $\boldsymbol{SD}$ and $\bar{\boldsymbol{X}}$ are standard deviation and mean values over the study period.

$$CV = \left(\frac{SD}{\bar{X}}\right) * 100 \tag{1}$$

2.3.2 Mann-Kendall test

The Mann-Kendall is the non-parametric statistical test for trend detection mostly used to examine increasing, decreasing or no-trend of rainfall time series. This method requires no prerequisite condition of the data and is normally applied to investigate the hydro-climatological data series in terms of spatial variation and temporal trends [12]. Many authors [13-15] have used this method to examine significant precipitation trends in different regions. The computation of the Mann-Kendall test considers n data time series containing two subsets of the data i and j where i = 1,2,3… n-1 and j = 1,2,3…n. These data are arranged in order time series and each one is compared to all subsequent data. Statistic S (Equation 2 and 3) is calculated and decreases if the data presented in a later period is lower than a data of a previous period and vice versa. The final set of S is all thus computational output.

$$S = \sum_{i=1}^{n-1} \sum_{j=i+1}^{n} sign(x_j - x_i) \tag{2}$$

$$sign(x_j - x_i) \begin{cases} +1 \; if \; (x_j - x_i) > 0 \\ 0 \quad if \; (x_j - x_i) = 0 \\ 0 \quad if \; (x_j - x_i) = 0 \end{cases} \tag{3}$$

Where x_i and x_j are annual precipitation of year i and j and $j > i$, respectively. n is the number of total data and $sign(x_j - x_i)$ is the result of equation 3 calculation. The standard normal statistic test (Z-test) is then calculated as Equation 4, whereas the variance of S can be computed using Equation 5

$$z \begin{cases} \frac{S-1}{\sqrt{Var(S)}} \; if \; S > 0 \\ 0 \; if \; S = 0 \\ \frac{S+1}{\sqrt{Var(S)}} \; if \; S < 0 \end{cases} \tag{4}$$

$$Var(S) = \frac{1}{18}[n(n-1)(2n+5) - \sum_{j=1}^{m} t_j(t_j - \quad 1)(\quad 2t_j + 5)] \tag{5}$$

Where n is the number of the tied group that is a zero difference between compared values and t_j is the number of data points in the t^{th} tied group. Positive / Negative Z value indicates an increasing/decreasing trend of precipitation.

2.3.3 Standardized Anomaly Index (SAI)

Standardized Anomaly Index (SAI) is commonly used to evaluate precipitation status in various areas [16-17, 10]. It was used to describe rainfall variability. The frequency of dry and wet incidents is also clarified by calculating annual rainfall events deviating from the average yearly rainfall in the study period. Negative\positive SAI values reflect less rainfall than normal, which is risky to drought\flood events. Equation 6 presents the method to compute SAI. x_i is the annual rainfall of year i and μ and δ is the average and standard deviation of long term rainfall period. SAI value can be classified into 7 groups indicated in Table 2.

$$SAI_i = \frac{(x_i - \mu)}{\delta} \tag{6}$$

Table 2 SAI classification

SAI	Category
2.0+	Extremely wet
1.5 to 1.9	Very wet
1.0 to 1.49	Moderately wet
-0.99 to 0.99	Near normal
-1.0 to -1.49	Moderately dry
-1.5 to -1.99	Severely dry
-2.0 and less	Extremely dry

3. Results and Discussion

Projected precipitation of ten GCMs according to AR6 climate change scenarios: SSP1-2.6, SSP2-4.5, SSP3-7.0 and SSP5-8.5, including historical simulation, were analyzed over the SEA region. Data in historical and scenarios simulations were considered during the 1850-2014 and 2015-2100 periods. Spatial precipitation variability, trend and condition grid by grid over the entire area are shown. The differences in precipitation characteristics among all ten models were revealed.

3.1 Precipitation variation of SEA under climate change scenarios

The coefficient of variation values (CV) of 10 GCMs with 5 scenarios (4 SSP (2015-2100) and historical simulations (1850-2014)) were calculated (Figure 2). CV was ranged in between 0-100% and then classified into three groups: Low (0-20%), Medium (20-30%) and High variation (>30%). Figure 2 presents all spatial distribution of CVs over SEA. During the historical period, high precipitation variation could be clearly seen in the six model outputs of CESM2, CMCC-CM2, CMCC-ESM2, NorESM2 TaiESM1 and MRI-ESM2. These models produced precipitation showing high variability in the southern and eastern parts of the region. In the south, high variability of precipitations had occurred in the Indian Ocean close to Indonesia. The North Pacific Ocean also exhibited high precipitation variation. The other models, GFDL, INM-CM4, INM-CM5, specified only a small area of high CV in the North Pacific Ocean. Only MPI-ESM1 presented high precipitation variability in the western and southern part of Thailand, west of Burma and some areas of the Philippines and Indonesia. Moderate precipitation variabilities were also presented with large regions of CESM2, CMCC-CM2, CMCC-ESM2, NorESM2 and TaiESM1and GFDL. CESM2 and NorESM2 simulated the moderate level in the area around the Philippine Sea, some parts of Vietnam, Indonesia and the Philippines; whereas CMCC-CM2, CMCC-ESM2, TaiESM1and GFDL exhibited moderate precipitation mostly in the South of SEA. Small areas of this level were also presented in INM-CM4, INC-CM5 and MPI-ESM1 located in the South of SEA.

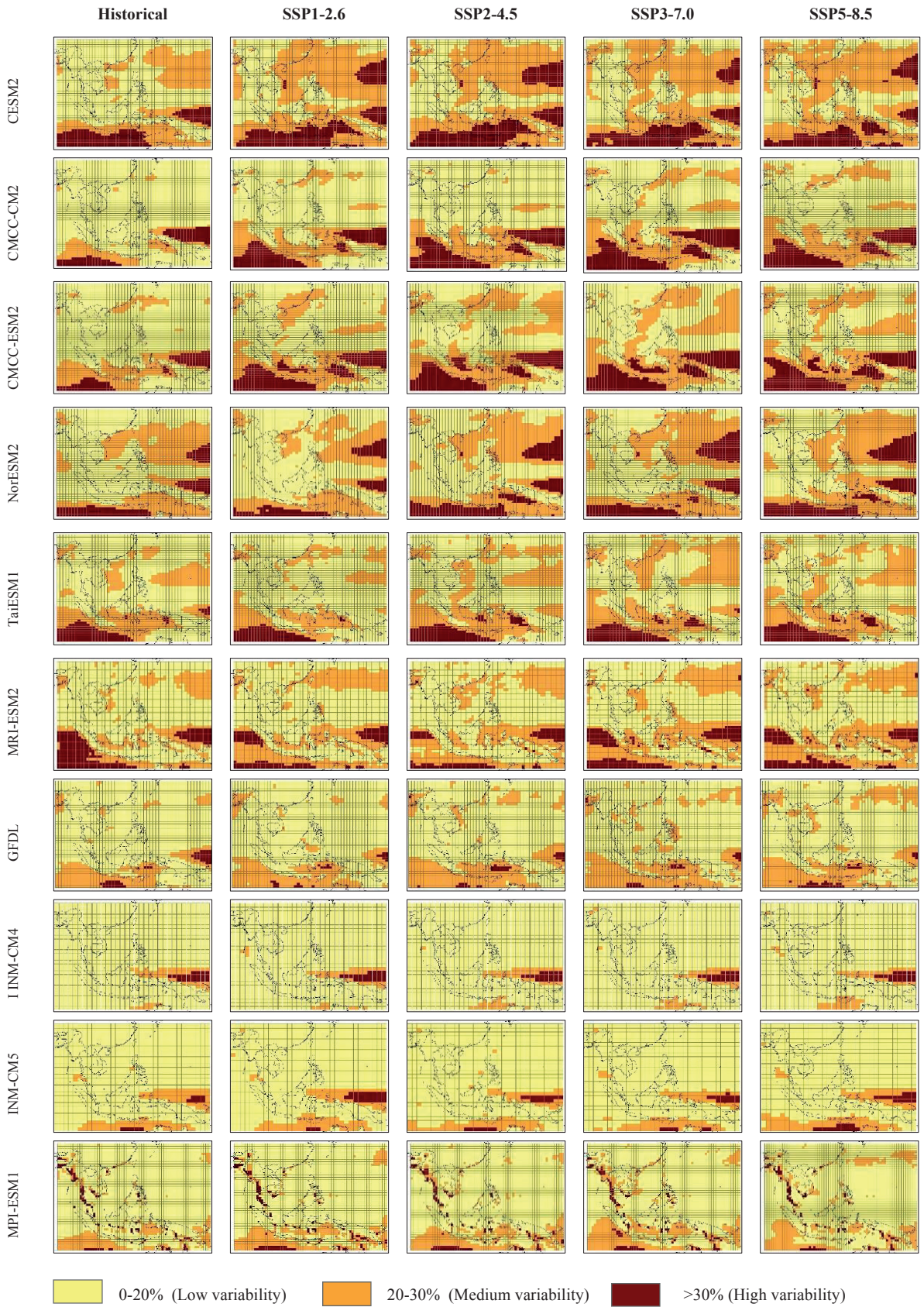

Figure 2. Spatial coefficient of rainfall variation over SEA (historical period: 1850-2014 / SSP: 2015-2100)

Projected precipitation under climate change scenarios using climate model strongly affected rainfall variability shown in CESM2 and NorESM2, especially for high levels of rainfall variation. CESM2 developed high rainfall variation in a larger area around the Philippines Sea and the Pacific Ocean in all SSP scenarios compared to the historical period showing no high variation around this area. NorESM2 also yielded similar results with a small area of high rainfall variation in these areas in the historical period. A larger coverage area could be seen for SSP scenarios. CMCC-CM2 and CMCC-ESM2 gave an increased range of CV around the Indian Ocean. A larger covering close to Indonesia could be noticeably found when four scenarios were forced into the models. Precipitation variation calculated from the other models during the historical period slightly differed from SSP scenarios.

In sum, if the spatial distribution of CVs were closely considered, it was found that GCMs could be divided into three groups. The first group, CESM2, CMCC-CM2, CMCC-ESM2, NorESM2, TaiESM1 and MRI-ESM2 mostly presented the highest CV in the same area with the same scenario. The second group was INM-CM4, INM-CM5 and GFDL showed a low level of CV in the large SEA area. Only small regions of the medium and high level of CV were found. Finally, MPI-ESM1 indicated a high variation of precipitation spread over in the mainland countries that were significantly different from others, as shown in Figure 2, with CV higher than 30% presenting in Thailand, Burma and some parts of Indonesia.

3.2 Precipitation trends of SEA under climate change scenarios

An overview of the spatial distribution of rainfall trends in SEA developed by 10 GCM models under historical and four SSP scenarios are shown in Figure 3. Statistical Z values were calculated for all grid cells across the region. Positive and negative values indicate an increase and decrease in rainfalls, respectively. The differences among the 10 model outputs could be noticed. In the historical simulations, CESM2 presented rainfall decreases in Burma, the North and the Northeast of Thailand, Laos, Cambodia, Vietnam and some parts of Malaysia and Indonesia similar to NorESM2, TaiESM1, MRI-ESM2, GFDL and INM-CM4. CMCC-CM2, CMCC-ESM2, INM-CM5 and MPI-ESM1 contradictorily showed rainfall increments in these countries.

Precipitation trends significantly changed when the models were applied with different scenarios. Increasing rainfalls were found in countries identified to have experienced rainfall decrease during historical periods (Burma, the North of Thailand, Laos, Cambodia, Vietnam, Malaysia, Indonesia, Brunei and Singapore) in CESM2 TaiESM1 and INM-CM4. In the scenario of SSP1-2.6, most models produced rainfall increases in most SEA countries except GFDL and MPI-ESM1. This event occurred in the Philippines, SEA and the Pacific. Increasing rainfalls for the entire region can be noticeably seen in TaiESM1 under SSP3-7.0 and SSP5-8.5, whereas SSP2-4.5 of this model and MPI-ESM1 under SSP1-2.6, SSP2-4.5 and SSP3-7.0 yielded rainfall decreases in most countries. These results were mostly consistent with [18], indicating a significant increase of precipitation under SSP5-8.5 rather than SSP2-4.5. All scenarios of MPI-ESM1exhibited a negative trend according to the Mann-Kendall test, while most of the Z results exhibited confidence intervals less than 90%.

3.3 SAI index of SEA rainfalls under climate change scenarios

SAI values of every year between 1850-2100 were calculated for all grid cells (Figures 4 and 5). SAI was initially categorized into seven classes. However, in this research it was modified to classify into three categories: very to extremely wet (SAI of higher than 1.5 to >2.0); severely to extremely dry (SAI of lower than -1.5 to <-2.0), and normal (SAI of -1.5 to 1.5) to mainly focus on extreme events of both wet and dry incidents. Percentages of events (a number of years) were calculated and compared to all years for the historical period (1850-2014: 165 years) and SSP scenarios (2015-2100: 86 years). Only extreme situations of both wet and dry events are explained below.

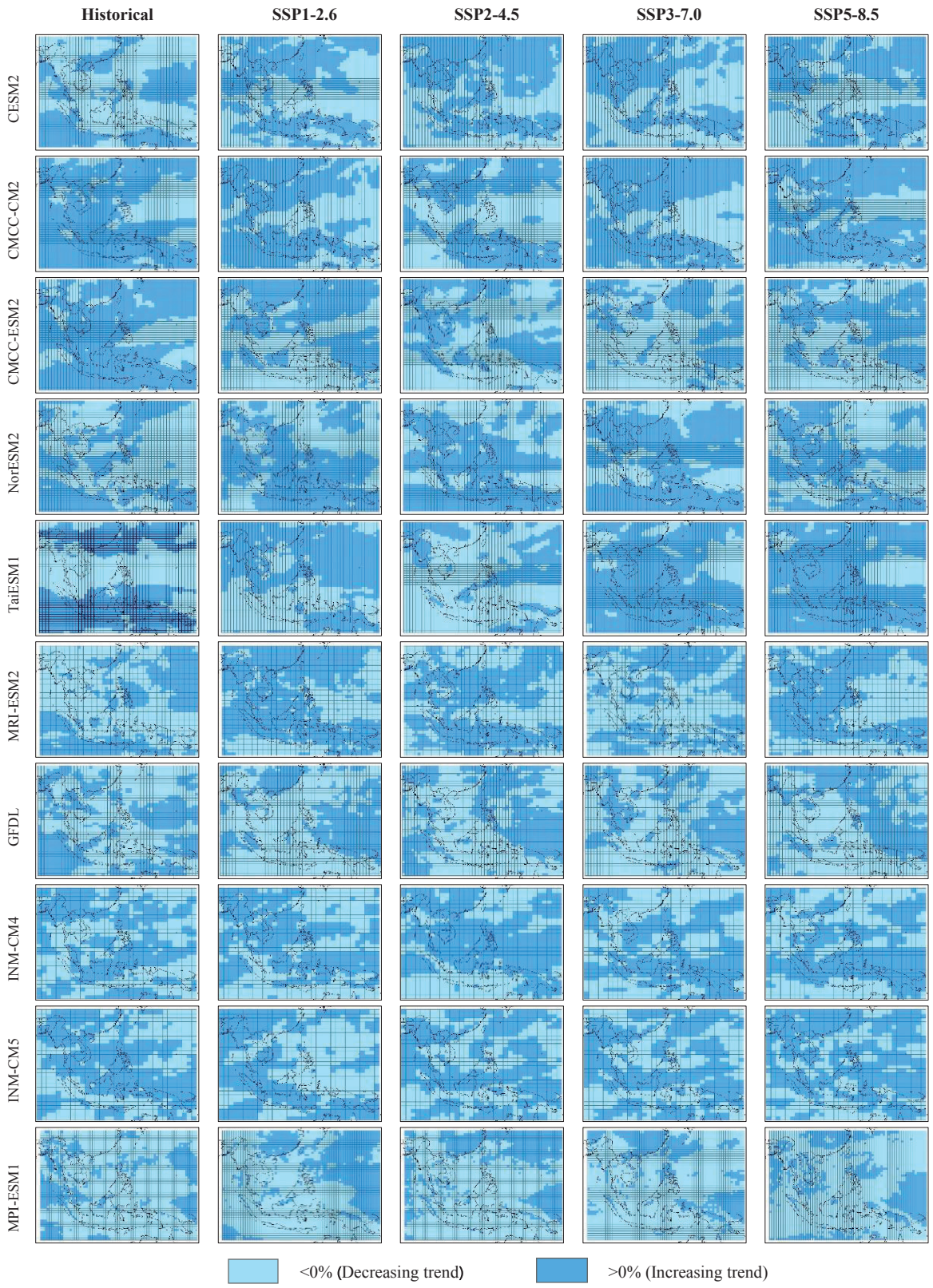

Figure 3. Spatial Mann-Kandell over SEA (historical period: 1850-2014 / SSP: 2015-2100)

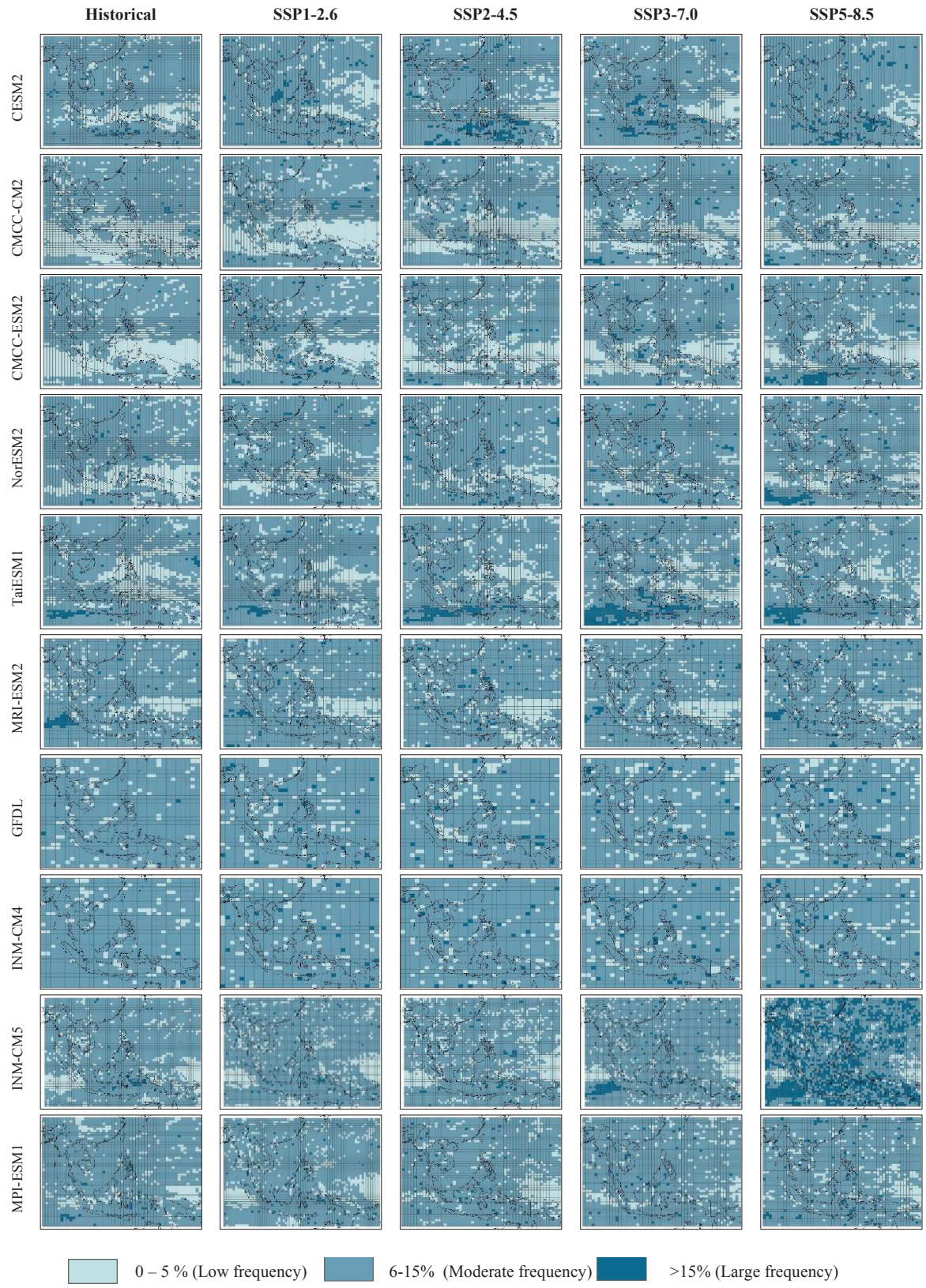

Figure 4. SAI very to extremely wet over SEA (historical period: 1850-2014 / SSP: 2015-2100)

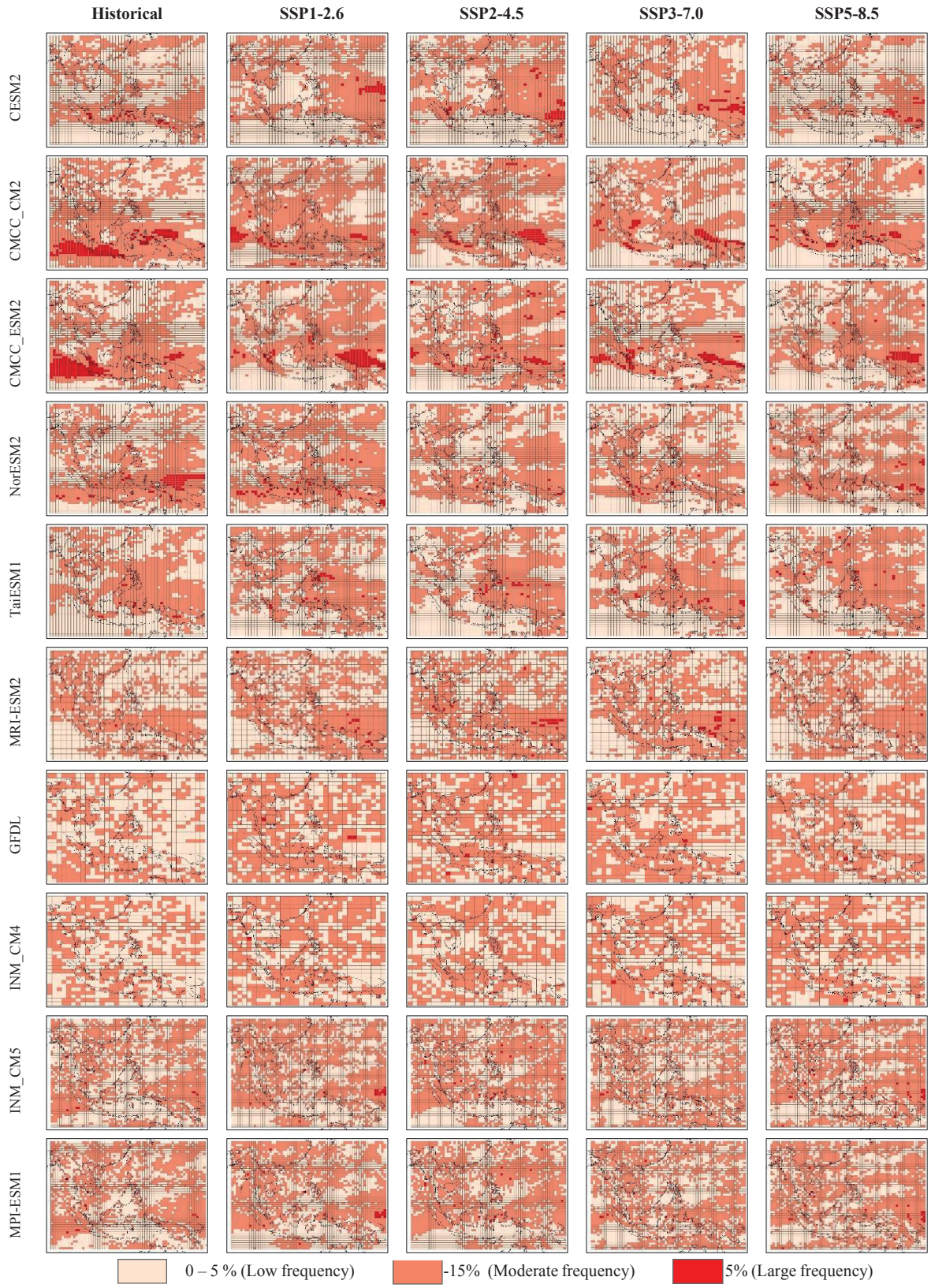

Figure 5. SAI severely to extremely dry over SEA (historical period: 1850-2014 / SSP: 2015-2100)

3.3.1 SAI-very to the extremely wet incident

The frequencies of rainfall conditions in very to extremely wet occurrences are shown in Figure 4. All precipitation simulations showed that very to extremely wet years often occurred in the range of 0-20% for all scenarios. However, most models simulated thefrequency of very to extremely wet occurrence for all over the region, around 6-15%, except the projection of INM-CM5 under SSP5-8.5, indicating this incident as more frequent than others. The differences of model simulation are noticeably presented. During the historical period, most countries faced extremely wet events in moderate frequency (6-15%) in various models except CESM2, CMCC-CM2, CMCC-ESM2 and NorESM2, showing a low-frequency level in most areas of Indonesia and the North Pacific Ocean. High precipitation events occurred with large frequency (>15%) in the Indian Ocean close to the West of Indonesia in TaiESM1 and MRI-ESM2.

Significant differences between historical periods and SSP scenarios were shown in various models. CESM2 exhibited a higher frequency of extreme events with more than 15% around the southern part of Indonesia with SSP2-4.5, SSP3-7.0 and SSP5-8.5, similar to TaiESM1. CMCC-ESM2 and NorESM2 presented a number of very-extreme wet with a high amount indicated in SSP5-8.5. Moderate frequency of these extreme events occurred covering most regions in GFDL and INM-CM4 in both historical period and SSP scenarios.

3.3.2 SAI-Severely to Extremely Dry conditions

A similar category of the events' frequency was also conducted with very to extremely dry conditions (Figure 5). Moderate frequency of drought conditions expanded all over the region for all models. CMCC-CM2, CMCC-ESM2, and NorESM2 historical simulations showed that extremely dry conditions often occurred around the South and West of Indonesia and the Indian Ocean. Countries in the mainland, for example, Thailand, Burma, Laos, Cambodia and Vietnam, mostly faced drought conditions during the historical period on a moderate scale (6-10%), resulting from most models.

According to climate change scenarios, SAI calculation showed a slight difference compared to the historical period. Moderate frequency of drought events occurred in large areas around the Philippines Oceans, whereas a small area of high frequency was also found for CESM2. CMCC-CM2 and CMCC-ESM2 gave a high frequency of drought conditions in the same area as CESM2. In contrast, the driest events around the South of Indonesia of these two models occurred in the historical period switched to the low and moderate frequency in all SSP scenarios. A large number of very to extremely dry incidents occurred across only a small area under climate change scenarios of NorESM2, TaiESM1 GFDL, MPR-ESM2 and MPI-ESM1.

4. Conclusions

Climate change's impact on various areas has been strongly evident, especially in Southeast Asia (SEA). The IPCC's sixth assessment report presents a future socio-economic projection of four scenarios for Tier1 with SSP1-2.6, SSP2-4.5, SSP3-7.0 and SSP5-8.5. This study investigated the difference of precipitation projection in spatial distribution under SSP scenarios and the historical period of ten models. These ten models had a spatial resolution of around 100 km with a variant label of r1i1p1f1. Variation, trend and condition of precipitations were analyzed using the coefficient of variation (CV), the Mann-Kendall test and Standardized Anomaly Index (SAI). Results revealed that significant differences between models were found. Six models (CESM2, CMCC-CM2, CMCC-ESM2, NorESM2 TaiESM1 and MRI-ESM2) clearly show high-moderate precipitation variation in the same area around the Indian Ocean and the North Pacific. These results were significantly different compared to the rest of the models. The Mann-Kendall test presented high variations among ten models. Eight models showed precipitation increments in most mainland countries for most scenarios except GFDL and MPR-ESM1. Finally, SAI was calculated for extremely wet and dry occurrences. The highest frequency of extremely wet events was seen with INM-CM5 under SSP5-8.5, whereas all models gave a majority range of extreme event occurrences around 6-10% of the study period. The increase of precipitation occurrences with extreme events in Southeast Asia were also found in [19]. Three models (CESM2, CMCC-CM2 and CMCC-ESM2) noticeably presented a high frequency of dry situation in variance from other models, which predominately showed only a low-moderate frequency of drought. The results of this study showed the differences among all ten models. Some models can be categorized in the same group whereas other GCMs presented significant differences. [20] also mentioned the performance difference among GCMs with different metrics. Therefore, researchers should pay more attention to selecting the output of

GCMs for continuing working on climate change areas. Considering a large number of GCMs or multi-model ensembles were recommended. This should notify researchers for model selection in the next step of local study on precipitation under climate change scenarios.

5. Acknowledgements

This study was supported by the Faculty of Engineering at Kamphaengsaen campus, Kasetsart University, Thailand. Also, the authors (s) would like to thank Dr. Winai Chaowiwat, a senior researcher (water resources engineering) at Hydro-Information Institute, for the valuable knowledge.

Author Contributions:

Funding: This research received no external funding

Conflicts of Interest: The authors declare no conflict of interest.

References

1. Asian Development Bank. The Economics of Climate Change in Southeast Asia: A Regional Review 2009; ISBN 978-971-561-787-1.
2. Hijioka, Y.; Lin, E.; Pereira, J.J.; Corlette, R.T.; Cui, X.; Insarov, G.E.; Lasco, R.D.; Lindgren, E.; Surjan, A. Asia. In: Climate Change: Impacts, Adaptation, and Vulnerability. Part B: Regional Aspects. Contribution of Working Group II to the Fifth Assessment Report of Intergovernment Panel on Climate Change 2014.
3. National Intelligence Council. Southeast Asia: The Impact of Climate Change to 2030: Geopolitical Implications. Conference Report CR 2010-02 January 2010.
4. Meinshausen, M.; Nicholls, Z.R.J.; Lewis, J.; Gidden, M.J.; Vogel, E.; Freund, M.; Beyerle, U.; Gessner, C.; Nauels, A.; Bauer, N.; Canadell, J.G.; Daniel, J.S.; John, A.; Krummel, P.B.; Luderer, G.; Meinshausen, N.; Montzka, S.A.; Rayner, P.J.; Reimann, S.; Smith, S.J.; Berg, M.; Velders, G.J.M.; Vollmer, M.K.; Wang, R.H.J. The shared socio-economic pathway (SSP) greenhouse gas concentration and their extensions to 2500. *Geoscientific Model Development.* 2020, 13, 3571-3605.
5. Fajardo, J.; Corcoran, D.; Roehrdanz, P.R.; Hannah, L.; Marquet P.A. GCM compareR: a web application to assess differences and assist in the selection of general circulation models for climate change research. *Methods in Ecology and Evolution.* 2020, 11, 656-663.
6. Raty, O.; Raisanen, J.; Ylhaisi, J. Evaluation of delta change and bias correction methods for future daily precipitation: intermodel cross-validation using Ensemble simulations. *Climate Dynamics.* 2014; 42, 2287-2303.
7. Charles J. V.; Douglas, E.M.; Green, P.A.; Revenga, C. Geospatial indicators of emerging water stress: an application to Africa. *Ambio.* 2005, *34*(3), 230-236.
8. Bekele, F.; Mosisa, N.; Terefe, D. Analysis of current rainfall variability and trends over Bale-Zone, South Eastern Highland of Ethiopia. *SF Journal of Global Warming.* 2017, 1:2.
9. Pujiastuti, I.; Nurjani, E. Rainfall pattern variability as climate change impact in the Wallacea Region. IOP Conf. Series: *Earth and Environmental Sciences.* 2017, 148. 012023.
10. Eshetu, G.; Johansson, T.; Garedew, W. Rainfall trend and variability analysis in Setema-Gatira area of Jimma, Southwestern, Ethiopia. *African Journal of Agricultural Research*. 2016, *11*(32), 3037-3045.
11. Archite, M.; Caloiero, T.; Walega, A.; Krakauer, N.; Hartanim T. Analysis of the spatiotemporal annual rainfall variability in the Wadi Cheliff Basin (Algeria) over the period 1970 to 2018. *Water.* 2021, 13, 1477.
12. John, A.S.; Brema, J. Rainfall trend analysis by Mann-Kendall test for Vamanapuram River basin, Kerala. *International Jounral of Civil Engineering and Technology*. 2018, *9*(13), 1549-1556.
13. Hussain, F.; Nabi, G.; Boota, M.W. Rainfall trend analysis by using the Mann-Kendall test & Sen's slope estimates: a case study of district Chakwak rain gauge, Barani area, Northern Punjab province, Pakistan. *Science International (Lahore).* 2015, *27*(4), 3159-3165.
14. Gadedjisso-Tossou, A.; Adjegan, K.L.; Kablan, A.K.M. Rainfall and temperature trend analysis by Mann-Kendall test and significance for rainfed cereal yields in Northern Togo. *Sci.* 2021, *3*(17). 1-20.
15. Ahmad, I.; Tang, D.; Wang, T.; Wang, M.; Wagan, B. Precipitation trends over time using Mann-Kendall and Spearman's rho tests in Swat River basin, Pakistan. *Advances in Meteorology*. 2015, 431860.

16. Koudahe, K.; Kayode, A.J.; Samson, A.O.; Adebola, A.A.; Djaman, K. Trend analysis in standardized precipitation index and standardized anomaly index in the context of climate change in Southern Togo. *Atmospheric and Climate Sciences.* 2017, 7, 401-423.
17. Bayable, G.; Amare, G.; Alemu, G.; Gashaw, T. Spatiotemporal variability and trends of rainfall and its association with Pacific Ocean Sea surface temperature in West Harerge zone, Eastern Ethiopia. *Environmental Systems Research*. 2021, *10*(7). 1-21.
18. Supharatid, S.; Nafung, J.; Aribarg, T. Projected changes in temperature and precipitation over mainland Southeast Asia by CMIP6 models. *Journal of Water and Climate Change.* 2021, doi.10.2166/wcc.2021.015.
19. Ge, F.; Zhu, S.; Luo, H.; Zhi, X.; Wang, H. Future changes in precipitation extremes over Southeast Asia: insights from CMIP6 multi-model ensemble. *Environmental Research.* 2021, 16, 024013.
20. Lqbal, Z.; Shahid, S.; Ahmed, K.; Wang, X. Evaluation of CIMP6 GCM rainfall in mainland Souteast Asia. *Atmospheric Research.* 2021, doi.10.1016/j.atmosres.2021.105525.